01,02

Numerical simulation of the superconducting sigma neuron design

© A.S. Ionin[1,2,4], S.V. Egorov[1], M.S. Sidelnikov[1], L.N. Karelina[1], N.S. Shuravin[1], M.M. Khapaev[1,3], V.V. Bolginov[1]

[1] Osipyan Institute of Solid State Physics, Russian Academy of Sciences, Chernogolovka, Russia
[2] Moscow Institute of Physics and Technology (National Research University), Dolgoprudny, Moscow Region, Russia
[3] Moscow State University, Moscow, Russia
[4] OOO „SP „Quant", Moscow, Russia

E-mail: sasha-ionin@mail.ru

Received April 18, 2024
Revised April 18, 2024
Accepted May 8, 2024

The results of numerical simulation of the distribution of superconducting currents in the prototype of an adiabatic sigma neuron, implemented in 2023 in the form of a multilayer thin-film structure over a thick superconducting screen, are presented. The calculation was carried out in the 3D-MLSI program, which allows taking into account the three-dimensional design of the experimental sample. A good agreement was obtained between the values of the intrinsic inductances of the sigma neuron parts and the previously obtained numerical estimates. It is shown that the superconducting screen does not provide sufficient independence of the neuron elements, which is expressed in non-zero values of the corresponding components of the inductance matrix. This corresponds to the available experimental data and requires generalization of previously proposed models of the stationary state of a superconducting sigma neuron. A method is proposed to compensate for the parasitic coupling of the input and readout elements of the neuron by changing the shape of the control line.

Keywords: superconductivity, Josephson effect, neuromorphic computing, thin-film structures, numerical modeling.

DOI: 10.61011/PSS.2024.07.58963.25HH

1. Introduction

The goal of developing the superconducting neuromorphic devices is a subject of interest for many researches because of the growing number of tasks and amount of processed data. One of the research areas is development of adiabatic neurons (see for example [1–10]) which comply with physical reversibility requirement, when the system in each moment of time is in a quasi-steady-state [9]. The main characteristic of the neuromorphic elements is a transfer function, i.e. dependence of the readout signal on the input one. In papers [1,3] a superconducting sigma-neuron was described which is a single-junction interferometer with part of its circuit shunted with an additional inductor to read the output signal (magnetic flux). The input signal is also a magnetic flux set in the receiving circuit. It was demonstrated that the transfer function of such structure can be close to a sigmoidal dependence, necessary for the implementation of a superconducting perceptron which is the most common type of the neural networks. A prototype of such device as a multi-film structure placed above the thick-layer superconducting screen was presented in paper [11]. In general, the experiments proved the general concepts of the theoretical studies [1,3], but demonstrated, the need for taking into account some additional factors, namely, the impact of the measurement process on the state of the sample and possibility of the magnetic flux transfer in between the circuit elements through the superconducting screen.

To provide a properly operating superconducting sigma-neuron it is crucial to design its elements with pre-specified inductances since the sigmoidal transfer function is implemented only if certain inductance relationships are met [3]. In paper [11] described the model problem formulae for the thin-film strip placed above the thick-layer superconducting screen (see [12], paragraph 10) were used to determine the inductances, while an unexpectedly high match of the transfer function coefficients with experimental results were observed. The unexpectedness was due to the use of non-evident phenomenological assumptions to account for indirect (cranked) shape of neuron elements. In view of this, numerical modeling may be used for a joint solution of Londons and Maxwell equations for the three-dimensional multi-layer sample structure. This study was initiated in paper [13] using software 3D-MLSI [14] which is currently the most available one for the users in Russia. The inductance of one of the sigma-neuron partial loops (sequential connection of two of three major parts of neuron), inductance of readout circuit and their mutual inductance were estimated.

However, these data are insufficient, since parametric form of the transfer function even for an isolated sigma-neuron (see. [3]) includes individual inductances of three neuron elements. To make approximation of the transfer function of a prototype sample [11] additional estimation of mutual inductances of control line with neuron receiving elements, as well as with measuring element (two-junction SQUID) is required. The objectives of this paper are to calculate the full inductance matrix of a practical sigma-neuron and demonstration of 3D-MLSI software capabilities for design of neuromorphic interferometry structures.

2. Methods

Sigma-neuron is a complex of inductive elements L_a, L and L_{out}, connected at one common point O and closed to screen in points A, B and C, respectively (see Figure 1). Compared to theoretical papers [1,3], „practical“ sigma-neuron (consisting of elements 2–4) is completed with a control line CL (element 1) used to set the input signal, and with a reading SQUID with a loop inductance L_{sq} (element 5). At points A and C the superconducting strip lines are closing directly to the screen through windows in the insulation layer, and connections at points B, D and E are made via tunnel Josephson junctions. The last circumstance has no effect on calculations of the inductance matrix components since they are defined by the configurations of flowing currents and do not depend on superconducting phase difference at the connection point. A more detailed description of the sigma-neuron structure and the technological process of its fabrication is given in article [11].

The studied sigma-neuron structure contains three superconducting layers located on various heights. First metal layer $M1$ (grey rectangular in Figures 1, 2) is a superconducting screen and a lower electrode for the neuron and measuring SQUID at the same time. Its thickness is 300 nm. In the second superconducting layer $M2$ most of the inductive elements (orange hatching with a slope to the right in Figure 1) is located. This layer is 100 nm thick and is separated from the screen surface with a 330 nm gap. The third layer $M3$ (red hatching with a slope to the left in Figure 1) is 450 nm thick and is separated from the screen with a 760 nm gap (composed of two 330 nm gaps and a second superconducting layer 100 nm thick). The overlap zone of the second and third layers is used for inductive coupling between the circuit elements (see Figure 2, *a*). In particular, the control line is coupled to the receiving elements L and L_a, and the SQUID loop is coupled to the element L_{out}. Based on the earlier developed drawing a file of input data describing a slightly simplified neuron structure for 3D-MLSI program was created. Major simplifying assumptions were the constant thickness of each of the layers, as well as their constant height above the screen (see Figure 2, *b*). The sample structure provides for 5 contacts between the layers $M1$ and $M2$ (A–E)

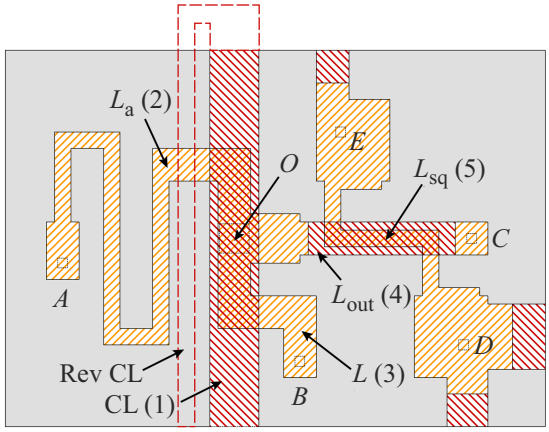

Figure 1. Schematic representation (top view) of investigated sigma-neuron structure. Designations are explained in the text. The number in parentheses indicates the number of row and column in the inductance matrix (see Table). The dotted line shows „reverse“ strip of control line (see discussion in Sect. 3).

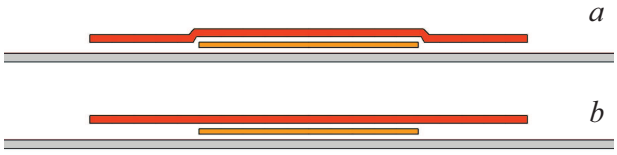

Figure 2. Schematic cross-section of stripline overlap areas above the superconducting screen (not to scale). The colors of layers correspond to Fig. 1: grey — $M1$ (bottom layer), orange — $M2$ (middle layer), red — $M3$ (upper layer). (*a*) Actual profile, (*b*) simulated (simplified) profile.

which ensure closure of the neuron or measuring SQUID elements to the superconducting screen to obtain closed superconducting circuits. At the point „O“ (see Figure 1) where neuron elements are connected a virtual contact (absent in reality) between the layers ($M1$ and $M2$) was located required to set individual currents into the neuron elements during computational modeling. The program simulated the supercurrent flowing along five current paths. The first one corresponds to the current flowing along a rectangular strip of the control line (CL) located entirely in layer $M3$ (red hatching with a slope towards left in Figure 1). Other four circuits (OAO, OBO, OCO and DED in Figure 1) were simulated as a ring closed through the superconducting screen via virtual or real contacts. It should be noted that paper [13] contained calculations of self-inductance and mutual inductance of ACA and DED circuits for a slightly different neuron elements geometry.

The calculation parameters are London penetration depth of 80 nm [15], as well as minimal and maximal grid spacing. The grid is formed in 3D-MLSI program automatically by means of a well-known triangular grids generator called Triangle [16]. Minimal grid spacing of 1 μm is applied near the edges of the superconducting structures

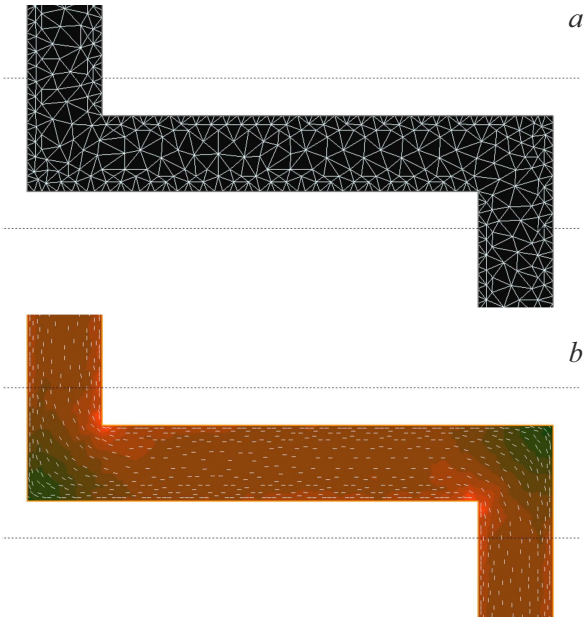

Figure 3. (a) Variable size triangular grid built for the SQUID loop (element 5 in Figure 1). (b) Calculated distribution of the supercurrent with its flowing through the SQUID loop. Lighter areas stand for higher current density. White dashes indicate the current direction.

(see Figure 3, a), where the value and direction of the supercurrent vary greatly in space (see Figure 3, b). With distance from the edges of the superconducting structures the grid spacing increased to 3 μm (see Figure 3, a) in order to reduce the number of triangles and computation time. Upon completion of computation we obtained distribution of the current density in layers of the thin-film structure, as well as an inductance matrix with a size of 5×5, containing self-inductances and mutual inductances of all reviewed elements. Because of its symmetrical nature the inductance matrix contains 15 various components at all. A detailed description of the mathematical model and computational methods used in 3D-MLSI program are given in papers [13,14]. The computation was made on AMD Ryzen 9 5900X 3.70 GHz processor in single-core mode.

To verify compliance of the 3D-MLSI modeling with the experiment the more simple structures were studied: single-loop double-junction interferometers manufactured as per the same process as in papers [11,17]. The interferometers had an U-shape structure (see Figure 4), at that, the interferometer loop was closed to the screen at the root of U-shape by means of tunnel Josephson junctions (JJ). Both JJ were shunted with 0.6 Ω resistance to provide their current-voltage curves to be singe-valued. Bias current of the sample was fed to the loop center (symmetrically) through the special bias line (top in Fig. 4) and removed through the superconducting screen. A special signal line („feedback line“, FB), was connected to SQUID loop allowing the current to flow through the interferometer loop

Inductance matrix of elements of the sigma-neuron prototype implemented in article [11]

L_{jk}, pH	1 (CL)	2 (L_a)	3 (L)	4 (L_{out})	5 (L_{sq})
1 (CL)	8.20	0.75	0.69	0.00	0.07
2 (L_a)	0.75	21.20	0.05	−0.05	0.00
3 (L)	0.69	0.05	2.65	0.05	0.00
4 (L_{out})	0.00	−0.05	0.05	5.91	−1.53
5 (L_{sq})	0.07	0.00	0.00	−1.53	7.64

and thus, creating a magnetic flux through it. The name was selected because similar line was used to set the feedback signal in the study of the superconducting neuron [11]. Under the cross-bar „of U-character“ laid the control line, CL, separated from it by a second layer of insulation.

The developed structure allowed to estimate both, the self-inductance L of SQUID loop, and mutual inductance M of sample with control line. For this, the so-called voltage-flux characteristic was measured: the periodic dependence of dc (averaged) voltage U occurring in SQUID in the non-stationary mode versus feedback line current I_{FB} (Figure 5, a) or control line current I_{CL} (Figure 5, b). The first method allows to define the self-inductance of the 2-junction interferometer as $L = \Phi_0/\Delta I_{FB}$ (Φ_0 — magnetic flux quantum, ΔI_{FB} — period of function $U(I_{FB})$), the

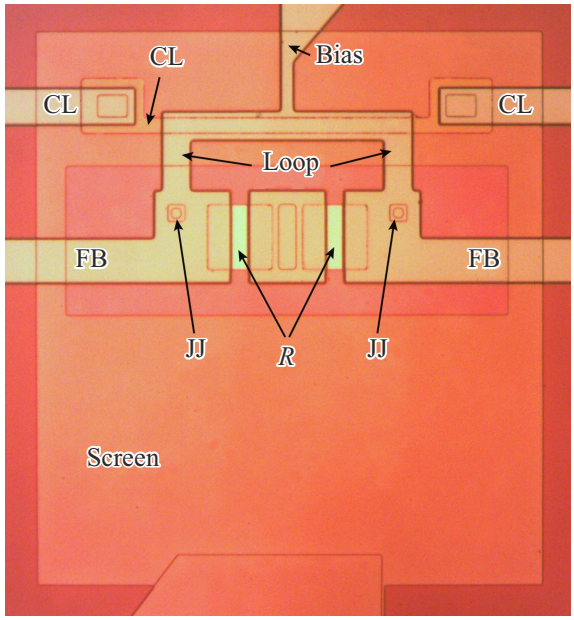

Figure 4. A micro-photo of test interferometer structure with overlap of the interferometer loop and control line. The interferometer loop is made in $M3$ layer and lies above the control line in $M2$ layer. The structure is formed above the superconducting screen. The scheme has the following designations (see definitions in the text): Josephson junctions JJ; shunting resistances R; bias line; feedback line FB and control line CL.

second method allows to define the mutual inductance of SQUID and control line as $M = \Phi_0/\Delta I_{CL}$. The periodicity of curves $U(I_{FB})$ and $U(I_{CL})$ follows from the resistively shunted junction (RSJ) model taking into account periodic dependence of critical current of the two-junction SQUID on the magnetic flux through its loop [12]. The obtained values L and M were compared with results of modeling in 3D-MLSI program where the geometry of sample in flat layers approximation was used (see Figure 2, *b*).

3. Results

Let us consider the results of experimental study of the single-loop double-junction interferometers. Figure 5 illustrates typical voltage-flux characteristics of samples obtained in 2 ways: when setting the signal from the feedback line and from the control line. The curves may be approximated by a sinusoidal dependence, with the accuracy of period determination based on the least-squares method better than 1%. The self-inductance of the loop is 10.0 pH, while mutual inductance is 3.3 pH. Numerical modeling provides values 10.5 pH for the self-inductance of the loop and 3.2 pH for the mutual inductance. Thus, actual and calculated inductance values coincide with an accuracy of 3–5%, which allows using 3D-MLSI software for modeling the superconducting neuron structure.

The major results are given in Table. The sigma-neuron elements are numbered „from the setting to reading element“, as shown in Figure 1. Self-inductances of the neuron elements are located in diagonal in the central submatrix 3×3 of the inductance matrix L_{ik} (see the Table). The diagonal element L_{55} corresponds to the inductance of the measuring SQUID. L_{11} element is a self-inductance of the control line and is not included in any of the sigma-neuron state equations, since the control line doesn't form a closed superconducting circuit. The interaction of the neuron with the measuring circuit is described by off-diagonal elements $L_{45} = L_{54}$, located on the outer ring as seen from the Table. Also the off-diagonal elements $L_{12} = L_{21}$, $L_{13} = L_{31}$ describing the input signal received from the control line are located there. Other components of the inductance matrix describe the parasitic interaction of neuron elements with each other. Some of them are distinctly non-zero and make 5–10% from the „useful“ off-diagonal components L_{12}, L_{13}, L_{45}.

It is interesting to compare the values of L_{ik} components with estimates in article [11] based on the model problem formulae concerning the strip line above the thick superconducting screen. The estimate values may be considered as reference since their use provided a good match of parameters of the experimental and calculated curves. The values of neuron elements self-inductance are matching with high accuracy (0.5–3.6%), however, lower values of the off-diagonal components are observed in computation compared to the model estimations. This may be caused by simplified geometry of the upper superconducting layer

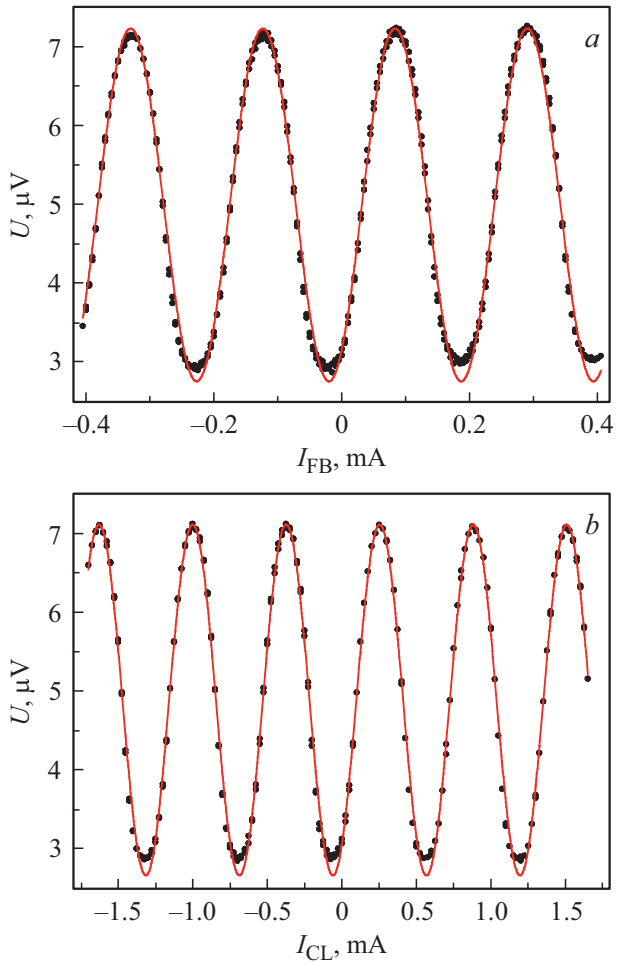

Figure 5. Voltage-flux characteristics of interferometer shown in Figure 4, and obtained by passing the control current through the feedback line (*a*) and through the control line (*b*). Points represent experimental data, red lines show approximation with a sinusoidal dependence used for determination of period. Bias current is 15 μA, the experiment temperature is 1.5 K.

during modeling or because of the technological flaws leading to higher actual mutual inductance. In particular, the calculated „useful“ off-diagonal components L_{12}, L_{13} (which define the period of the transfer function) and component L_{45} (which defines the output signal change amplitude) are lower than the estimates by 6–15%. In spite of the same shape of the receiving sections, the input magnetic flux is unsymmetrical in the neuron receiving arms ($L_{12} \neq L_{13}$), which is contradicting to one of the assumptions in theoretical papers [1–3]. The reason for this may be the non-uniform effect of the „closing currents“ in the superconducting screen (see [11] and discussion below) on L and L_a inductances, which are hugely different in terms of their form (see Figure 1). So far, this circumstance, as well as parasitic off-diagonal components, have not been taken into account in construction of theoretical models.

Calculations also demonstrated that the superconducting screen cannot provide a full independence of the sigma-

neuron elements from each other, which was supposed in theoretical models [1–3]. Thus, a non-zero value of L_{15} was confirmed, which directly transmits the input signal to the measuring circuit. The calculated value is approximately by 30% lower of the estimate value [11], though they are of the same order of magnitude (0.1 pH). Apart from L_{15} component, quite high values were obtained from the off-diagonal components L_{23}, L_{24} and L_{34} which describe the interaction of neuron elements L, L_a and L_{out}. Zero value of component L_{14} describing the interaction of the control line (CL) with the output inductance L_{out}, can be expected because L_{out} element is located perpendicular to the control line on the screen symmetry axis. Zero values of coefficients L_{25}, L_{35} are beneficial but unexpected, because the measuring SQUID loop (element 5 in Figure 1) has sections parallel to the corresponding neuron elements (elements 2 and 3 in Figure 1). Currently, we do not exclude reduction of the off-diagonal components because of simplification of the simulated structure. The testing and improvement of existing program is a subject of our ongoing research.

Among the parasitic off-diagonal components, the most harsh is L_{15} component describing the direct interaction of control line with the measuring circuit. It is this line which is responsible for the appearance of additional linear component which obstructs the implementation of the target sigmoidal [11] or Gaussian [17] transfer function. Figure 6 shows an example of distribution of currents in the screen which occur there when the current flows through the control line. It is demonstrated that in the superconducting screen a „back-flow“ current arises under the control line (1) which has to be closed through the rest part of the screen. The closing currents have a component along the receiving SQUID circuit (5) which causes the „parasitic“ direct transfer of the input magnetic flux into it. Thus, the results of numerical modeling prove the qualitative analysis given in paper [11].

The presence of parasitic coupling of the inductance elements through the superconducting screen was observed also for the test double-junction interferometers. Figure 7 shows a micro-photo of the superconducting interferometer without overlap of the SQUID loop and control line. However for their mutual inductances the value $M = 0.12$ pH was obtained in the experiment (see Figure 8, *a*). Computation in 3D-MLSI program gives a value of 0.18 pH. The experimental value of the self-inductance of the interferometer loop was $L = 13.6$ pH (see Figure 8, *b*), and value calculated in 3D-MLSI — 14.1 pH. Thus, we may see a good match (3–5%) of the experiment and 3D-MLSI modeling results for 1–10 pH inductance, and a reasonable estimate for inductances of the order of 0.1 pH. The inductances of the order of 1 fH were rounded to zero in Table. The discrepancies noted above can also be associated with the technological flaws. Currently, the testing of 3D-MLSI program using samples manufactured at a higher process level takes place.

The lower effect of closing currents may be reached by adding into the neuron structure a control line's „reverse“ part located near the main one and through which I_{CL} current is flowing in reverse direction. For this purpose the control line may be arranged in the form of a half-loop (see the dash line in Figure 1). In this case the closing currents are concentrated in the gap between the main and reverse strips (see Figure 9), and in the outer area

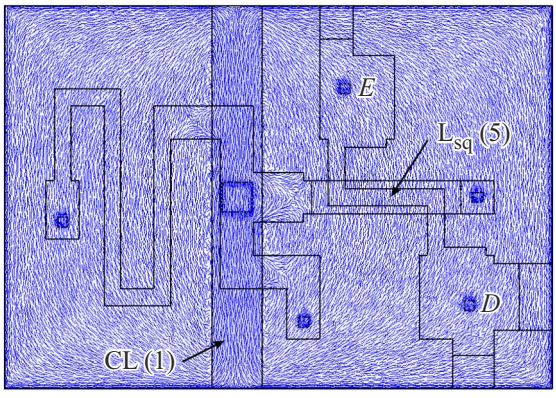

Figure 6. The calculated distribution of currents in the screen when the current flows through the control line. Blue dashes indicate the current direction.

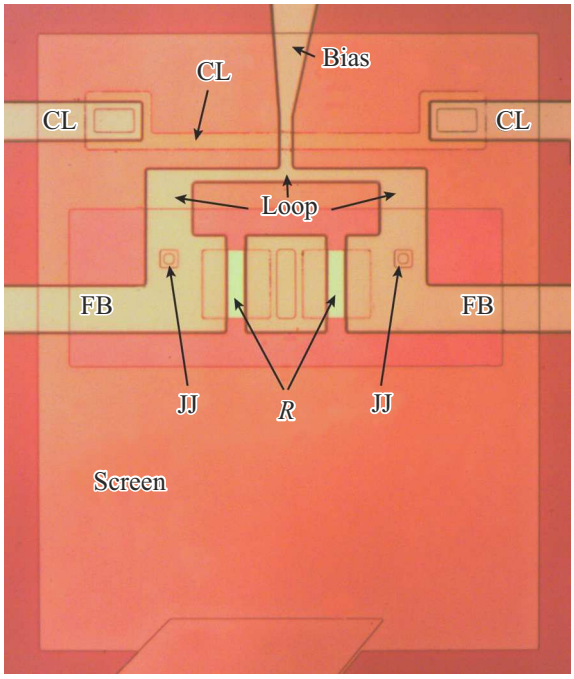

Figure 7. A micro-photo of test interferometer structure without overlap of the interferometer loop and control line. The interferometer loop is made in layer $M3$ and lies on the side of the control line in layer $M2$. The structure is formed above the superconducting screen. The scheme has the following designations (see definitions in the text): Josephson junctions JJ; shunting resistances R; bias line; feedback line FB and control line CL.

they become much weaker. Computation using 3D-MLSI program for such geometry shows reduction of L_{15} in five times. To preserve constant the „useful“ components of the inductance matrix, the „reverse“ strip shall have no any overlap of the neuron elements, though it may cross them. Apart from suppression of L_{15} component, the use of bi-directional control line slightly increases components L_{12} (by 12%) and L_{13} (by 5%) leaving the other off-diagonal components unchanged. The change of components L_{12} and L_{13} indicates the connection between their asymmetry ($L_{12} \neq L_{13}$) and the flow of closing currents as described above. In general, the increase of L_{12} and L_{13} is beneficial, since it allows to reduce the transfer function period on control current (see discussion in [11]). This asymmetry may be compensated by a slight increase of the length of the overlap zone of the element L with the control line (see Figure 1). Thus, the suggested method of suppressing the parasitic input signal transfer to the receiving circuit doesn't require any significant modification of sigma-neuron design.

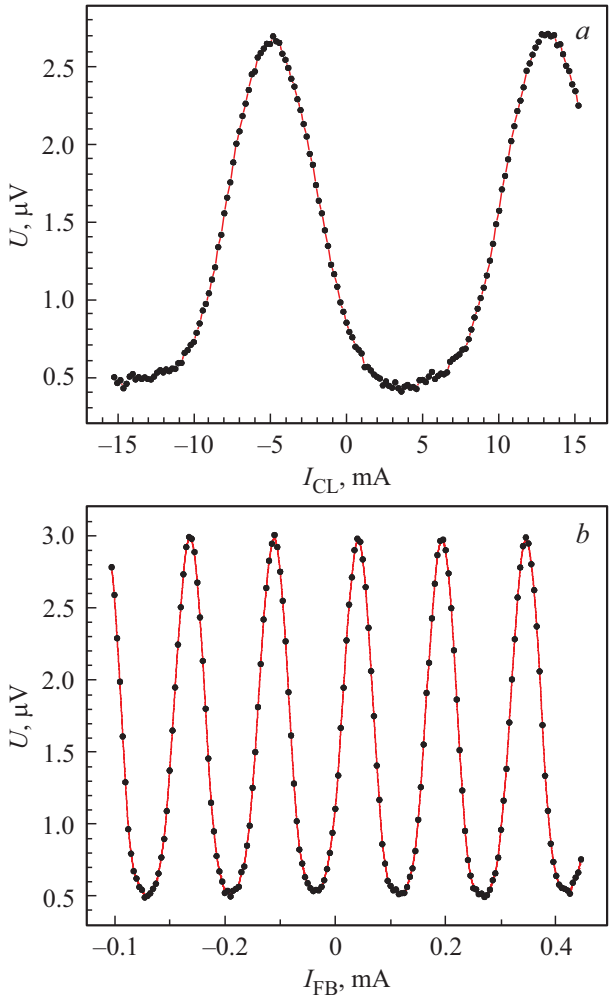

Figure 8. Voltage-flux characteristics of interferometer shown in Figure 7, and obtained by passing the control current through the control line (a) and through the feedback line (b). Bias current is 9 μA, experiment temperature is 1.5 K.

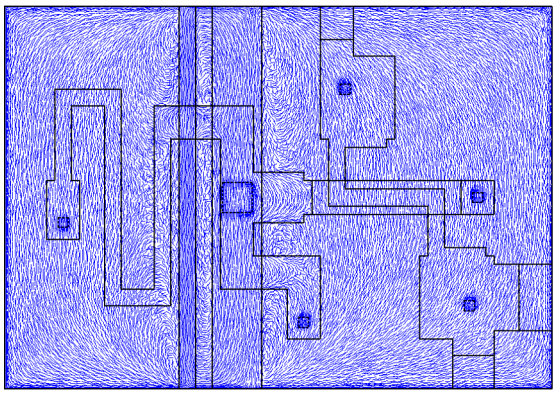

Figure 9. The calculated distribution of currents in the screen when the current flows through the bi-directional control line. Blue dashes indicate the current direction.

4. Conclusion

The inductances matrix was calculated for the superconducting sigma-neuron prototype based on the Londons and Maxwell equations in 3D-MLSI program. The applicability of 3D-MLSI program to deal with the specified task was demonstrated by comparing the calculated and experimental measured values of self-inductances and mutual inductances of the thin-film double-junction interferometers formed above the superconducting screen. The superconducting screen was found as uncapable to provide the appropriate independence of the neuron elements, and a mechanism of direct transfer of the input signal to the receiving circuit through ring superconducting currents occurring as a response to the input magnetic flux has been confirmed. A method to minimize this effect using a bi-directional control line was suggested. Asymmetry of the input signal was found in the partial circuits of neuron with identical geometry of receiving sections, as well as the presence of other parasitic neuron elements couplings. The obtained results demonstrate the need for development of a generalized model of a stationary sigma-neuron state to allow for all off-diagonal inductance matrix components for analysis of experimental data and design of the next generation superconducting neurons.

Funding

The computation of the superconducting sigma-neuron inductance matrix and analysis of obtained results were performed in the Institute of Solid State Physics, Russian Academy of Science under the grant of the Russian Science Fund (RSF) No. 23-72-00053. Double-junction interferometers were produced within the framework of the production practice of graduate student A.S. Ionin — from the Moscow Institute of Physics and Technology. The research works on the double-junction interferometers was carried out within cooperation with JV Quant, LLC. Calculation of self-inductances and mutual inductances of

interferometers was performed within the works schedule of associate professor M.M. Khapaev — Lomonosov Moscow State University (department of computational methods in computational mathematics and cybernetics division).

Conflict of interest

The authors declare that they have no conflict of interest.

References

[1] A.E. Schegolev, N.V. Klenov, I.I. Soloviev, M.V. Tereshonok. Beilstein J. Nanotechnol. **7**, 1397 (2016).
[2] N.V. Klenov, A.E. Schegolev, I.I. Soloviev, S.V. Bakurskiy, M.V. Tereshonok. IEEE Trans. Appl. Supercond. **28**, *7*, 1301006 (2018).
[3] I.I. Soloviev, A.E. Schegolev, N.V. Klenov, S.V. Bakurskiy, M.Yu. Kupriyanov, M.V. Tereshonok, A.V. Shadrin, V.S. Stolyarov, A.A. Golubov. J. Appl. Phys. **124**, 152113 (2018).
[4] A.E. Schegolev, N.V. Klenov, I.I. Soloviev, A.L. Gudkov, M.V. Tereshonok. Nanobiotechnology Rep. **16**, *6*, 811 (2021).
[5] A.E. Schegolev, N.V. Klenov, I.I. Soloviev, M.V. Tereshonok. Supercond. Sci. Technol. **34**, *1*, 015006 (2021).
[6] M.V. Bastrakova, A. Gorchavkina, A.E. Schegolev, N.V. Klenov, I.I. Soloviev, A.M. Satanin. Symmetry (Basel). **13**, *9*, 1735 (2021).
[7] A.E. Schegolev, N.V. Klenov, S.V. Bakurskiy, I.I. Soloviev, M.Yu. Kupriyanov, M.V. Tereshonok, A.S. Sidorenko. Beilstein J. Nanotechnol. **13**, 444 (2022).
[8] M.V. Bastrakova, D.S. Pashin, D.A. Rybin, A.E. Schegolev, N.V. Klenov, I.I. Soloviev, A.A. Gorchavkina, A.M. Satanin. Beilstein J. Nanotechnol. **13**, 653 (2022).
[9] I.I. Soloviev, G.S. Khismatullin, N.V. Klenov, and A.E. Schegolev. J. Commun. Technol. Electron. **67**, 1479 (2022).
[10] D.S. Pashin, P.V. Pikunov, M.V. Bastrakova, A.E. Schegolev, N.V. Klenov, I.I. Soloviev. Beilstein J. Nanotechnol. *14*, 1116 (2023).
[11] A.S. Ionin, N.S. Shuravin, L.N. Karelina, A.N. Rossolenko, M.S. Sidel'nikov, S.V. Egorov, V.I. Chichkov, M.V. Chichkov, M.V. Zhdanova, A.E. Shchegolev, and V.V. Bol'ginov. JETP **137**, 888 (2023).
[12] V.V. Schmidt. *The Physics of Superconductors: Introduction to Fundamentals and Applications* (MTsNMO, Moscow, 2000; Springer, Berlin, 1997).
[13] S.V. Bakursky, N.V. Klenov, M.Yu. Kupriyanov, I.I. Soloviev, M.M. Khapaev. Computation mathematics and mathematical physics **61**, 854 (2021).
[14] M.M. Khapaev, A.Y. Kidiyarova-Shevchenko, P. Magnelind, M.Y. Kupriyanov. IEEE Trans. Appl. Supercond. **11**, *1*, 1090 (2001).
[15] A.I. Gubin, K.S. Il'in, S.A. Vitusevich, M. Siegel, N. Klein. Phys. Rev. B **72**, *6*, 064503 (2005).
[16] J.R. Shewchuk. Comput. Geom. Theory Appl. **22**, *1–3*, 21 (2002).
[17] A.S. Ionin, L.N. Karelina, N.S. Shuravin, M.S. Sidel'nikov, F.A. Razorenov, S.V. Egorov, and V.V. Bol'ginov. JETP Letters **118**, 766 (2023).

Translated by T.Zorina